SCIENCE CHINA
Information Sciences

• RESEARCH PAPER •

November 2013, Vol. 56 112202:1–112202:9
doi: 10.1007/s11432-013-5009-0

# Biped walking on level ground with torso using only one actuator

FENG Shuai[1,2], Al Yahmadi Amur S.[3] & SUN ZengQi[1]*

[1]*State Key Laboratory of Intelligent Technology and Systems, Tsinghua National Laboratory for Information Science and Technology, Department of Computer Science and Technology, Tsinghua University, Beijing* 100084*, China;*
[2]*Beijing Institute of Control Engineering, Beijing* 100190*, China;*
[3]*Department of Mechanical and Industrial Engineering, College of Engineering, Sultan Qaboos University Al-Khod 123* P.O. Box 33*, Sultanate of Oman*

Received May 3, 2013; accepted August 7, 2013

**Abstract** It is well known that a biped robot needs actuators to walk stably on level ground. Till now, a biped robot with torso has needed at least two actuators to achieve this. Would it be possible for this kind of robot to walk on level ground with only one actuator? This paper responds in the affirmative and proposes a simple control strategy for a planar biped robot with torso. In this control method, there is only one low gain proportional-derivative (PD) controller between the torso and the stance leg, while the swing leg remains totally free. The PD controller utilizes states of both the torso (angle and angular velocity) and the stance leg. The numerical simulations show that, by adopting this controller, a planar biped robot with torso can walk stably on level ground, and that the robot can walk with a wide range of speeds and high energy efficiency by changing the control parameters. Four period-one gaits, one of which is stable while the other three are unstable, are found by simulations. According to the literature surveyed, we are the first to have a torso only driven biped robot walk stably on level ground.

**Keywords** biped robot, torso control, passive dynamic walking, PD controller

**Citation** Feng S, Al Yahmadi A S, Sun Z Q. Biped walking on level ground with torso using only one actuator. Sci China Inf Sci, 2013, 56: 112202(9), doi: 10.1007/s11432-013-5009-0

## 1 Introduction

McGeer pioneered the study of passive-dynamic walking [1]. He showed, by analysis of linearized models and construction of dynamic mechanisms, that a biped robot without actuators and controllers can walk stably down a shallow slope. In this motion, the energy lost when the swing foot hits the ground is recovered by gravitational potential energy. Thus, a fully passive dynamic walker can only walk down a slope.

To realize level-ground walking, active power, replacing gravity, must be injected into the biped robot. McGeer proposed various methods [2–4], including 1) applying torque at the ankle and hip joints, 2) applying an impulsive push as the stance leg leaves the ground, 3) varying the leg length, and 4) utilizing

*Corresponding author (email: szq-dcs@tsinghua.edu.cn)

 

reaction torque against a leaning torso. Although many studies have adopted the first control method for level-ground walking [5–8], there are relatively few papers on the fourth control method. From an aesthetic perspective, it is natural for a biped robot to have a torso. Moreover, from an engineering perspective, many instruments can be added onto the torso, thereby greatly expanding the application scope of a biped robot. As such, it is important to include and control the torso of a biped robot. Till now, researchers have mainly adopted one of the following three ways of adding or controlling the torso.

1) Utilizing purely mechanical equipment. The proponents of this method are Wisse and Gomes. In 2007, Wisse [9] used a kinematic coupling mechanism to keep the torso midway between the two legs. However, his robot, controlled only by this mechanism, can only walk down a slope. In Gomes' model [10], two legs are connected to the torso by torsional springs. This model can walk on level ground with no energy cost, but it cannot be considered to be formally stable.

2) Utilizing a "hard" control method to specify that the torso angle remains constant throughout the step, which is referred to as a "perfectly stabilized torso" in McGeer's paper [3]. In 1998, Howell [11] investigated gait behavior of a torso-driven biped model. In his research, the torso was kept parallel to the surface of the ground throughout the stride. In 2005, using a "perfectly stabilized torso", Narukawa [12] showed two period-one gaits, which were found with the torso near vertical. However, this kind of control method is not exact, since an impulsive stance/torso torque, which would need to be calculated precisely, would be required at support transfer [13].

3) Utilizing a "soft" control method or mechanism, which means that the torso can sway to a certain extent. The typical controller of this method is a proportionate-derivative (PD) controller. In 2001, Harnua [13] placed a PD controller between the robot's stance leg and torso to keep the torso at a desired angle, while the swing leg was left free. This robot model can walk down a slope. Narukawa [4] incorporated swing leg control to enable the robot to walk on level ground. Besides the torso control, Hobbelen [14] also used ankle control to allow the robot to walk on level ground.

In summary, according to the literature surveyed, a biped robot with torso can walk stably down a slope using one actuator, but it needs at least two realizable actuators to walk on level ground. Narukawa [4] even mentioned that it was difficult for the biped robot to walk stably with only a low-gain PD controller to hold the torso.

It is obvious that using fewer actuators in the robot reduces the complexity and improves the reliability of the robot control system significantly. Thus, we tried to use as few actuators as possible to make a biped robot with torso walk stably on level ground. Is it possible for this kind of robot to walk on level ground using only one actuator? Providing an answer to this question is the motivation for this study. Fortunately the answer is positive.

First, we developed a simple control strategy for a planar biped robot with torso. In this strategy, there is only one PD controller between the torso and stance leg, while the swing leg remains totally free. This controller utilizes both the torso states (angle, angular velocity) and those of the stance leg. The numerical simulations show that, by adopting this controller, a biped robot is able to walk stably on level ground. Thereafter, we searched both the stable and unstable gaits and analyzed the influence of the control parameters.

## 2 Robot model

A simple biped robot with torso [15], as shown in Figure 1, is considered in this paper. The biped robot, confined to the sagittal plane, is composed of two identical rigid legs and a torso, which are connected at the hip. The biped robot has four point masses. The torso mass is denoted as $m_u$, each leg has mass $m_l$, and the hip has mass $m_h$. The length of the legs is $l = l_a + l_b$ and the torso length is $l_u$. Dynamic variables $\theta_1$, $\theta_2$, $\theta_3$ are measured from ground normal. In the robot system, there is only one control torque, which is applied between the torso and the stance leg. The values of the robot parameters are shown in Table 1.

A single typical step in the model is composed of a swing phase and a collision phase. In the swing phase, only the stance foot makes contact with the ground without slipping. In the collision phase, which

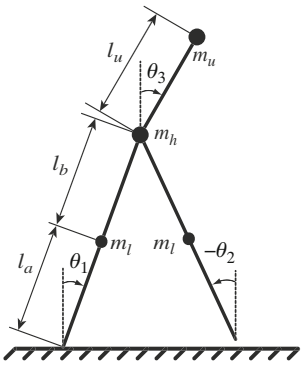


**Figure 1** Schematic of the robot model.

**Table 1** Values of robot parameters

| Parameter | Value | Unit |
|---|---|---|
| $m_u$ | 10 | Kg |
| $m_h$ | 10 | Kg |
| $m_l$ | 5 | Kg |
| $l_u$ | 0.5 | m |
| $l_b$ | 0.5 | m |
| $l_a$ | 0.5 | m |
| $g$ | 9.81 | m/s$^2$ |

is thought to be instantaneous, the swing foot touches the ground and the swing leg becomes the new stance leg, and vice versa.

### 2.1 Swing phase

During the swing phase, the stance foot acts as a pivot joint, while the scuffing problem of the swing foot is ignored. The dynamic equation of the robot system can be written as

$$\boldsymbol{M}(\boldsymbol{\theta})\ddot{\boldsymbol{\theta}} + \boldsymbol{N}(\boldsymbol{\theta}, \dot{\boldsymbol{\theta}}) + \boldsymbol{G}(\boldsymbol{\theta}) = \boldsymbol{B}u, \tag{1}$$

where $\boldsymbol{\theta} = (\theta_1, \theta_2, \theta_3)^{\mathrm{T}}$, and $u$ is the torque applied between the torso and stance leg. Details of the matrices are

$$\boldsymbol{M}(\boldsymbol{\theta}) = \begin{bmatrix} M_{11} & M_{12} & M_{13} \\ M_{21} & M_{22} & M_{23} \\ M_{31} & M_{32} & M_{33} \end{bmatrix}, \quad \boldsymbol{N}(\boldsymbol{\theta}, \dot{\boldsymbol{\theta}}) = \begin{bmatrix} N_1 \\ N_2 \\ N_3 \end{bmatrix}, \quad \boldsymbol{G}(\boldsymbol{\theta}) = \begin{bmatrix} G_1 \\ G_2 \\ G_3 \end{bmatrix}, \quad \boldsymbol{B} = \begin{bmatrix} -1 \\ 0 \\ 1 \end{bmatrix},$$

$M_{11} = (m_u + m_h + m_l)(l_a + l_b)^2 + m_l l_a^2$, $M_{12} = M_{21} = -m_l(l_a + l_b)l_b \cos(\theta_1 - \theta_2)$, $M_{13} = M_{31} = m_u(l_a + l_b)l_u \cos(\theta_1 - \theta_3)$, $M_{22} = m_l l_b^2$, $M_{23} = M_{32} = 0$, $M_{33} = m_u l_u^2$; $N_1 = -m_l(l_a + l_b)l_b \sin(\theta_1 - \theta_2)\dot{\theta}_2^2 + m_u(l_a + l_b)l_u \sin(\theta_1 - \theta_3)\dot{\theta}_3^2$, $N_2 = m_l(l_a + l_b)l_b \sin(\theta_1 - \theta_2)\dot{\theta}_1^2$, $N_3 = -m_u(l_a + l_b)l_u \sin(\theta_1 - \theta_3)\dot{\theta}_1^2$; $G_1 = -((m_h + m_l + m_u)(l_a + l_b) + m_l l_a)g \sin(\theta_1)$, $G_2 = m_l l_b g \sin(\theta_2)$, $G_3 = -m_u l_u g \sin(\theta_3)$.

### 2.2 Collision phase

A collision happens when the swing foot touches the ground. On level-ground walking, the collision occurs when the geometric condition

$$\theta_1 + \theta_2 = 0 \tag{2}$$

is satisfied. Eq. (2) is also true at least once when the legs are nearly parallel, but we ignore the scuffing and let the swing leg swing through without collision.

During the collision, the mechanical configuration remains unchanged, and the swing leg becomes the new stance leg, and vice versa. It is reasonable to assume that the collision is completely inelastic and that the new swing leg has no impulsive reaction with the ground as it leaves. Neglecting non-impulsive forces at collision, angular momentum is conserved through the collision for: 1) the whole robot system about the swing foot contact point, 2) the torso about the hip, and 3) the new swing leg about the hip. These angular momentum conservation relations give the following "jump" equation, where the "+" superscript means "just after collision", and the "−" superscript means "just before collision":

$$\begin{bmatrix} \mathbf{I} & \mathbf{0} \\ \mathbf{0} & \boldsymbol{H}^n(\boldsymbol{\theta}^+) \end{bmatrix} \begin{bmatrix} \boldsymbol{\theta}^+ \\ \dot{\boldsymbol{\theta}}^+ \end{bmatrix} = \begin{bmatrix} \boldsymbol{Q} & \mathbf{0} \\ \mathbf{0} & \boldsymbol{H}^o(\boldsymbol{\theta}^-) \end{bmatrix} \begin{bmatrix} \boldsymbol{\theta}^- \\ \dot{\boldsymbol{\theta}}^- \end{bmatrix}, \tag{3}$$

where $\dot{\boldsymbol{\theta}} = (\dot{\theta}_1, \dot{\theta}_2, \dot{\theta}_3)^{\mathrm{T}}$, and $\mathbf{I}$, $\boldsymbol{Q}$, $\boldsymbol{H}^n(\boldsymbol{\theta}^+)$ and $\boldsymbol{H}^o(\boldsymbol{\theta}^-)$ are 3-by-3 matrices, with $\mathbf{I}$ the identity matrix.

$$\boldsymbol{Q} = \begin{bmatrix} 0 & 1 & 0 \\ 1 & 0 & 0 \\ 0 & 0 & 1 \end{bmatrix}, \quad \boldsymbol{H}^n(\boldsymbol{\theta}) = \begin{bmatrix} H^n_{11} & H^n_{12} & H^n_{13} \\ H^n_{21} & H^n_{22} & H^n_{23} \\ H^n_{31} & H^n_{32} & H^n_{33} \end{bmatrix}, \quad \boldsymbol{H}^o(\boldsymbol{\theta}) = \begin{bmatrix} H^o_{11} & H^o_{12} & H^o_{13} \\ H^o_{21} & H^o_{22} & H^o_{23} \\ H^o_{31} & H^o_{32} & H^o_{33} \end{bmatrix},$$

$H^n_{11} = -(m_h + m_l + m_u)(l_a + l_b)^2 - m_l l_a^2 + m_l(l_a + l_b) l_b \cos(\theta_1^+ - \theta_2^+) - m_u(l_a + l_b) l_u \cos(\theta_1^+ - \theta_3^+)$, $H^n_{12} = m_l l_b (l_a \cos(\theta_1^+ - \theta_2^+) - l_b + l_b \cos(\theta_1^+ - \theta_2^+))$, $H^n_{13} = -m_u l_u (l_u + l_a \cos(\theta_1^+ - \theta_3^+) + l_b \cos(\theta_1^+ - \theta_3^+))$, $H^n_{21} = -m_u(l_a + l_b) l_u \cos(\theta_1^+ - \theta_3^+)$, $H^n_{22} = 0$, $H^n_{23} = -m_u l_u^2$, $H^n_{31} = m_l(l_a + l_b) l_b \cos(\theta_1^+ - \theta_2^+)$, $H^n_{32} = -m_l l_b^2$, $H^n_{33} = 0$, $H^o_{11} = m_l l_a l_b - (m_h + m_u)(l_a + l_b)^2 \cos(\theta_1^- - \theta_2^-) - 2m_l(l_a + l_b) l_a \cos(\theta_1^- - \theta_2^-) - m_u(l_a + l_b) l_u \cos(\theta_1^- - \theta_3^-)$, $H^o_{12} = m_l l_a l_b$, $H^o_{13} = -m_u l_u (l_u + l_a \cos(\theta_2^- - \theta_3^-) + l_b \cos(\theta_2^- - \theta_3^-))$, $H^o_{21} = -m_u(l_a + l_b) l_u \cos(\theta_1^- - \theta_3^-)$, $H^o_{22} = 0$, $H^o_{23} = -m_u l_u^2$, $H^o_{31} = m_l l_a l_b$, $H^o_{32} = 0$, $H^o_{33} = 0$.

## 3 Control method

To hold the torso, which is an inverted pendulum, active stabilization is required. In this paper, a simple PD controller has been developed as follows:

$$u = K_p(\theta^d - (\theta_3 - \theta_1)) - K_d(\dot{\theta}_3 - \dot{\theta}_1), \tag{4}$$

where $\theta^d$ is the desired angle, $K_p$ and $K_d$ are proportional gain and derivative gain, respectively, and $u$ is the torque applied between the torso and the stance leg. This controller provides a damped spring acting against the stance leg. The calculation of $K_p$ and $K_d$ given below is partly the same as that mentioned in [3].

The legs are assumed to be kept firmly vertical, which means $\theta_1 = \theta_2 = 0$ and $\dot{\theta}_1 = \dot{\theta}_2 = 0$. With the controller mentioned above, the linearized equation of the torso about $\theta_3 = 0$, $\theta^d = 0$ becomes $m_u l_u^2 \ddot{\theta}_3 + K_d \dot{\theta}_3 + (K_p - m_u l_u g)\theta_3 = 0$. The frequency of the torso is $\omega_T = \sqrt{K_p - m_u l_u g/(m_u l_u^2)}$, while the damping ratio is $\zeta_T = K_d/(2m_u l_u^2 \omega_T)$. With the damping ratio set as $\zeta_T = 0.7$, $K_p$ and $K_d$ can be calculated as

$$K_p = m_u l_u^2 \omega_T^2 + m_u l_u g, \tag{5}$$

$$K_d = 1.4 m_u l_u^2 \omega_T. \tag{6}$$

The controller can be parameterized by $\omega_T$ and $\theta^d$ . In our control, $\omega_T$ is relatively small, and therefore, the PD gains $K_p$ and $K_d$ are small and the robot's motions are largely natural and not overly controlled.

## 4 Performance criteria

The main performance criteria for biped walking under consideration in this paper are stability, walking speed, and specific cost.

### 4.1 Stability

By numerically integrating the equations of the stance and collision phases, the initial state $\boldsymbol{q} = (\boldsymbol{\theta}, \dot{\boldsymbol{\theta}})^{\mathrm{T}}$, which is the state of the biped robot just after the collision, can be mapped from one step onto the next step by a step-to-step function or the so called "stride function" $S$ [1,16]

$$\boldsymbol{q^{n+1}} = S(\boldsymbol{q^n}). \tag{7}$$

A state $\boldsymbol{q^*}$ is called a fixed point if it satisfies $\boldsymbol{q^*} = S(\boldsymbol{q^*})$, which means that if $\boldsymbol{q^*}$ is taken as the initial state, the biped robot will generate a periodic motion.

A Jacobian matrix, $\boldsymbol{J}$, can be defined as:

$$\boldsymbol{J} = \left.\frac{\partial S(\boldsymbol{q})}{\partial \boldsymbol{q}}\right|_{\boldsymbol{q}=\boldsymbol{q}^*}. \tag{8}$$

If all the Jacobian's eigenvalues are inside the unit circle, the fixed point is stable. If any eigenvalues of the Jacobian are outside the unit circle, the fixed point is unstable. In our biped system, the Jacobian is a 6-by-6 matrix, so it has 6 eigenvalues. In this paper, we are mainly concerned with the maximum amplitude of the eigenvalues. Details of the stability definition can be found in [1,17].

### 4.2 Walking speed

The average walking speed is defined as

$$v = \frac{\Delta x}{T}, \tag{9}$$

where $\Delta x$ is the step length and $T$ is the step period.

### 4.3 Specific cost

To compare the efficiency of humans and robots of different sizes, it is convenient to use the dimensionless specific cost of transport [18]. The dimensionless specific cost, used in this paper, is defined as

$$c_s = \frac{\int_0^T |(\dot{\theta}_3 - \dot{\theta}_1)u|\mathrm{d}t}{(m_u + m_h + 2m_l)g\Delta x}, \tag{10}$$

where $T$ is the step period, $g$ is the gravitational acceleration, and $\Delta x$ is the step length.

## 5 Simulations and results

Our primary investigation tool is numerical simulation. Using ODE113 to run the simulation in MATLAB, we specified a tolerance of 1e-8 for our numerical simulations. Collisions were detected by the EVENT function in ODE113, while the FSOLVE function in MATLAB was used to find the fixed point.

### 5.1 Typical stable walking

Figure 2 shows typical stable walking with $\theta^d = -0.07$ rad, and $\omega_T = 5.5$. The step period is 0.8527 s, the maximum absolute eigenvalue is 0.4614, the average speed is 0.6345 m/s, and the specific cost is 0.04435.

According to (4), it seems that the goal of the controller is to keep a desired angle $\theta^d$ between the torso and the stance leg. However, as shown in the Figure 2(b), there is an obvious difference between $\theta_3 - \theta_1$ and the desired angle $\theta^d$. The reason for this is that $K_p$ and $K_d$ are relatively small ($K_p = 124.675$, $K_d = 19.25$), compared to the value in [12] ($K_p = 490$, for the same robot structure). The torso is controlled rather softly, so that the jerk at collision is followed by a pronounced forward sway and recovery.

Using this low gain controller, instead of trying to keep the torso upright [14], we use the swing motion of the torso as a way of injecting energy into the robot system, and therefore, we allow the torso to swing slightly, though the swing motion is quite small (between 0.006 rad and 0.16 rad as shown in Figure 2(b)).

The angular velocity of the torso changes instantaneously in the collision, as can be seen in Figure 2(d). This is an inevitable result of the angular momentum conservation for the torso about the hip. Moreover, there is an impulsive energy loss of about 3 J in the collision (as shown in Figure 2(f)).

### 5.2 Stable and unstable gaits

Both stable and unstable period-one walking motions are found. By repeating the simulations and gradually changing the control parameter $\theta^d$, we obtained the comparison of the four motions shown in Figure 3. In these simulations, $\omega_T = 5.5$.

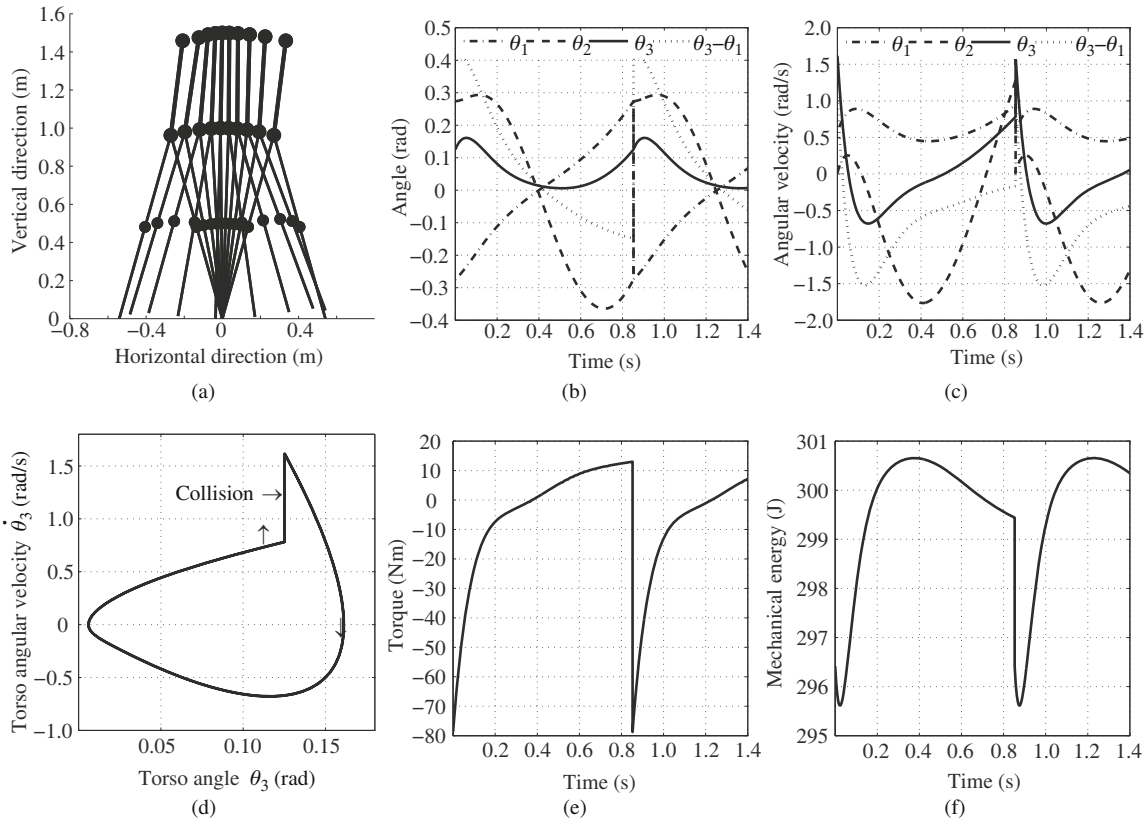


**Figure 2** Stable walking simulation results. (a) Stick diagrams of stable walking; (b) angular position; (c) angular velocity; (d) phase diagram of torso; (e) control torque; (f) mechanical energy.

In Figure 3, the solid line (Gait A) is the stable motion, while the others are unstable motions. The initial inter-leg angle in Figure 3(b) is the angle between the swing leg and the stance leg just after the collision in the periodic walking motion.

From Figure 3 (d) and (f), it can easily be deduced that Gait A and Gait B fall on the same curve, while Gait C and Gait D fall on a different curve. In Figure 3(c), the step periods of Gait A and Gait B are longer than those of Gait C and Gait D. The reason for this is that there is swing leg retraction in Gait A and Gait B, which means that the swing leg moves backwards just prior to foot collision, and thus takes more time. The retraction can be seen by comparing Figures 2(b) and 4, which shows Gait C with $\theta^d = -0.07$ rad and $\omega_T = 5.5$.

As shown in Figure 3(b), the step lengths of Gait A and Gait C are nearly the same when $\theta^d$ is the same and so are those for Gait B and Gait D. But because of the difference in step periods, the speeds for Gait C and Gait D, which are without swing leg retraction, are faster as shown in Figure 3(d). Figure 3 (b) and (e) shows that, as the step length increases, so too does the specific cost. This is true for all four gaits, because a longer step length results in a larger collision and induces more energy dissipation in a similar way to the motion of a rimless wheel [1]. Owing to the long periods, Gait A and Gait B have to adopt big steps to achieve the same walking speed as Gait C and Gait D, resulting in greater energy dissipation. This is why the curve of Gait A and Gait B is above the curve of Gait C and Gait D in Figure 3(f).

### 5.3 Effect of parameters

The influence of $\omega_T$ and $\theta^d$ in the stable period-one walking motion is considered in this section through a large numbers of simulations. In these simulations, four different $\omega_T$ values (4.5, 5.5, 6.5, and 7.5) were selected, and $\theta^d$ was gradually changed. The simulation results are shown in Figure 5.

Based on the graphs in this figure, the following can be concluded.

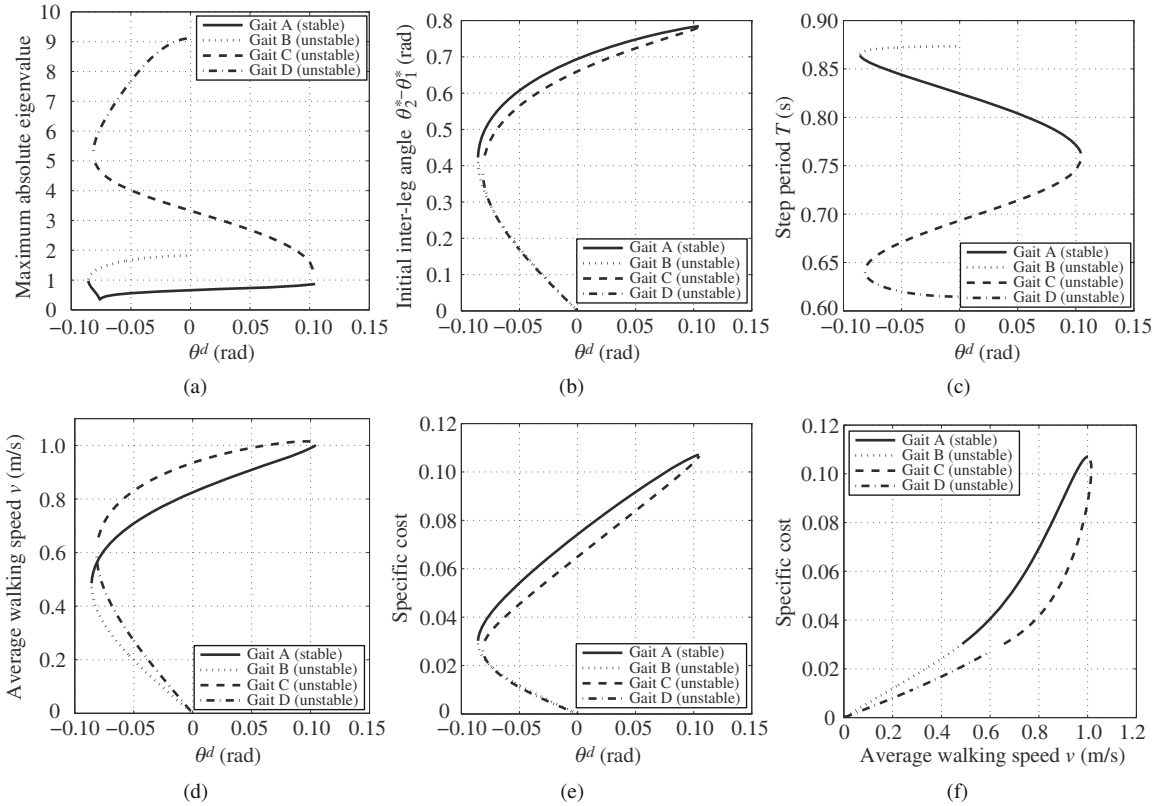


**Figure 3** Comparison of stable and unstable gait motion. (a) Maximum absolute eigenvalue; (b) initial inter-leg angle; (c) walking period; (d) average walking speed; (e) specific cost; (f) specific cost versus average walking speed.

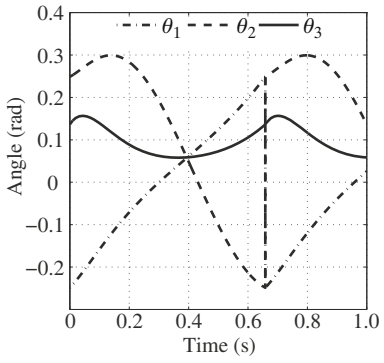


**Figure 4** Angular position of biped robot for Gait C.

1) The effect of $\theta^d$ in our system is similar to that of the slope in McGeer's synthetic wheel [1]. When $\theta^d$ increases, the step period decreases while the step length increases. The reason for this is that when $\theta^d$ becomes larger, the gravitational moment of the whole robot system about the support foot is larger, and therefore the rotation about the stance foot is faster, resulting in a shorter period. Moreover, because the moment is larger, the energy injected into the robot increases, and so the robot needs a larger step, which causes a greater collision that consumes more energy. Figure 6 clearly shows the inference. The Y-axis in Figure 6 is the angular velocity of the stance leg, which is an indication of the robot system's rotation. It should be noted that the time is normalized on the X-axis to show the comparison clearly. In this comparison, $\omega_T = 5.5$.

2) When $\omega_T$ increases, both the step period and step length increase. The reason for this is that as $\omega_T$ becomes greater, the torso recovers more quickly after the collision happens, and thus the gravitational moment is smaller, so the robot can rotate about the stance more slowly, which in turn, results in a longer

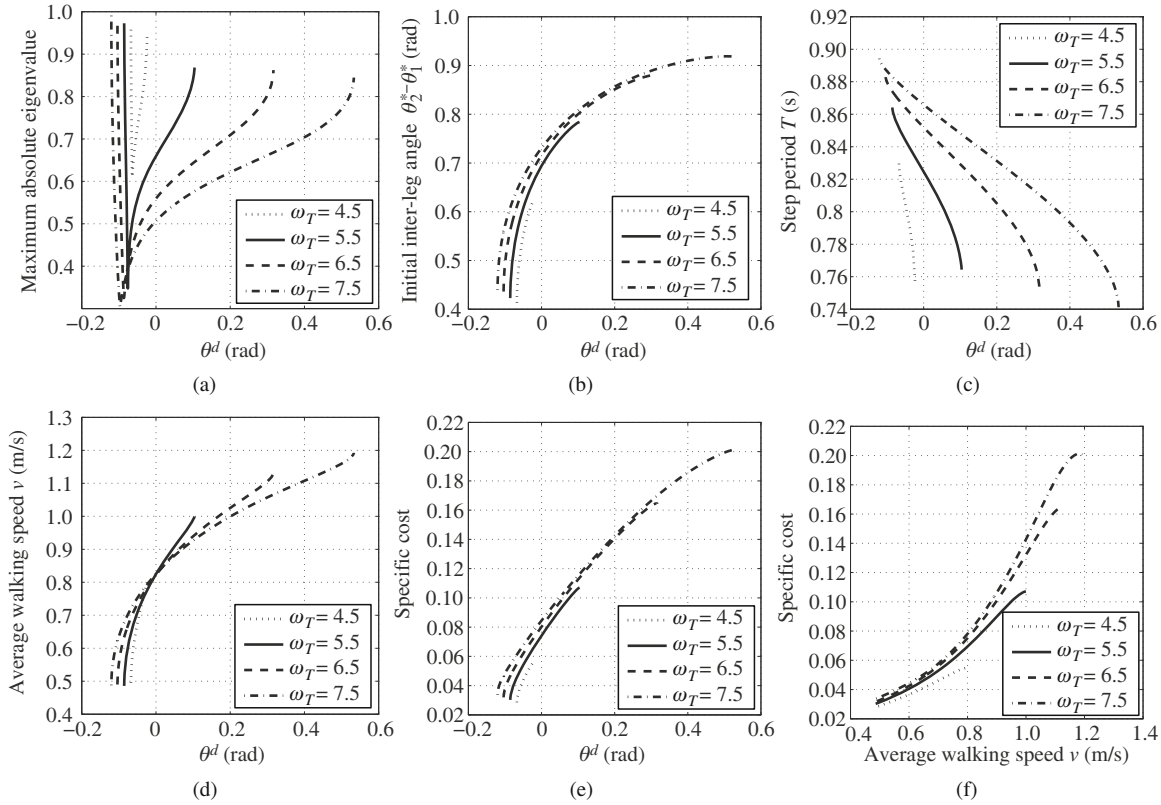


**Figure 5** Influence of $\omega_T$ and $\theta^d$ on stable walking motion. (a) Maximum absolute eigenvalue; (b) initial inter-leg angle; (c) walking period; (d) average walking speed; (e) specific cost; (f) specific cost versus average walking speed.

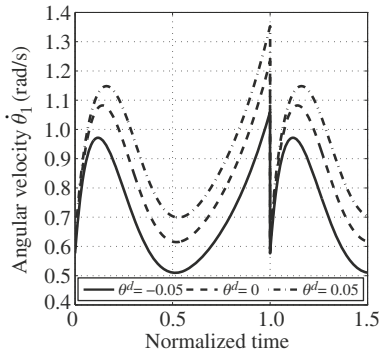


**Figure 6** Comparison of different $\theta^d$ values.

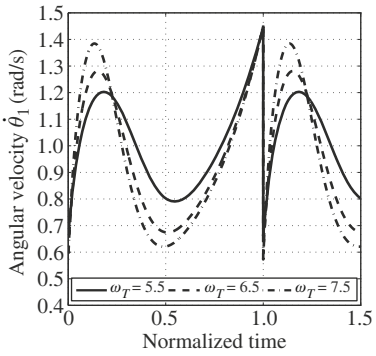


**Figure 7** Comparison of different $\omega_T$ values.

period. As the $\omega_T$ increases, the controller does more work, which leads to the larger step as mentioned before. From Figure 7, it is easy to see that a large $\omega_T$ generates a slow rotation after the the recovery of the torso. In this comparison $\theta^d = 0.1$ rad.

## 6 Conclusion

It is obvious that using fewer actuators in a robot can significantly reduce the complexity and increase the reliability of the robot control system. Thus, we attempted to use as few actuators as possible to make a biped robot with torso walk stably on level ground. As reported in this paper, we have succeeded in implementing stable level-ground walking for this type of robot using only one actuator. Because robots need at least one actuator to recover the energy lost in the collision, the minimal number of actuators is one. To the best of our knowledge, we are the first to achieve this.

In this paper, we introduced the control strategy for a planar biped robot with torso. In this control method, one low gain PD controller that utilizes the states of the torso and the stance leg, is applied between the torso and the stance leg while the swing leg remains totally free. The numerical simulations show that the robot can walk stably on level ground using this controller, and that by changing the control parameters, the biped robot with torso can walk with a wide range of speeds and high energy efficiency.

We analyzed the four period-one gaits found by simulations. We also analyzed the influence of the control parameters and found that as $\theta^d$ increases, the step period decreases while the step length increases. Moreover, when $\omega_T$ increases, both the step period and step length increase.

Our future work will focus on optimizing the control parameters to generate more efficient gaits.

**Acknowledgements**

We would like to express our deepest gratitude to Professor Ruina at Cornell University for his assistance, and to his students Petr and Pranav, who helped ensure that the simulations were correct and accurate.

## References

1 McGeer T. Passive dynamic walking. INT J Robot Res, 1990, 9: 62–82
2 McGeer T. Stability and control of two-dimensional biped walking. Technical Report CSS-IS TR 88-01, Simon Fraser University. 1988
3 McGeer T. Dynamics and control of bipedal locomotion. J Theor Biol, 1993, 163: 277–314
4 Terumasa N, Masaki T, Kazuo Y. Numerical simulations of level ground walking based on passive walk for planar biped robots with torso by hip actuators. J Syst Des Dyn, 2008, 2: 463–474
5 Ambarish G, Bernard E, Ahmed K. Limit cycles in a passive compass gait biped and passivity-mimicking control laws. Auton Robots, 1997, 4: 273–286
6 Spong M W, Bullo F. Controlled symmetries and passive walking. IEEE Trans Automat Contr, 2005, 50: 1025–1031
7 Fumihiko A, Minoru H, Norihiro K, et al. Extended virtual passive dynamic walking and virtual passivity-mimicking control laws. In: International Conference on Robotics and Automation, Seoul, 2001. 3139–3144
8 Fumihiko A, Masaki Y, Norihiro K, et al. A novel gait generation for biped walking robots based on mechanical energy constraint. IEEE Trans Robotic Autom, 2004, 20: 565–573
9 Martijn W, Daan G E H, Arend L S, et al. Adding an upper body to passive dynamic walking robots by means of a bisecting hip mechanism. IEEE Trans Robot, 2007, 23: 112–123
10 Gomes M W, Andy R. A walking model with no energy cost. Phys Rev E, 2011, 83: 032901
11 Howell G W, Baillieul J. Simple controllable walking mechanisms which exhibit bifurcations. In: IEEE Conference on Decision and Control, Tampa, 1998. 3027–3032
12 Narukawa T, Takahashi M, Yoshida K. Biped locomotion on level ground by torso and swing-leg control based on passive-dynamic walking. In: IEEE/RSJ International Conference on Intelligent Robots and Systems, Edmonton, 2005. 4009–4014
13 Masaki H, Masaki O, Koh H, et al. Yet another humanoid walking—passive dynamic walking with torso under simple control. In: International Conference on Intelligent Robots and Systems, Hawaii, 2001. 259–264
14 Hobbelen D G E. Limit cycle walking. Dissertation for the Doctoral Degree. Delft: Delft University of Technology, 2008
15 Jesse W G, Gabriel A, Franck P. Asymptotically stable walking for biped robots: Analysis via systems with impulse effects. IEEE Trans Automat Contr, 2001, 46: 51–64
16 Martijn W. Essentials of dynamic walking. Dissertation for the Doctoral Degree. Delft: Delft University of Technology, 2004
17 Ambarish G, Bernard E, Ahmed K. Limit cycles and their stability in a passive bipedal gait. In: International Conference on Robotics and Automation, Minneapolis, 1996. 246–251
18 Steve C, Andy R, Russ T, et al. Efficient bipedal robots based on passive-dynamic walkers. Science, 2005, 307: 1082–1085